Supplemental material for LHCb-PAPER-2022-013

Systematic Uncertainties

The systematic uncertainties from various sources are classified into three categories and are summarized in Tables 1 – 3. The first systematic uncertainty is associated with the normalization. The second type is point-to-point uncertainties where the uncertainty in each data point moves up or down independently. The uncertainties of the third type are correlated between data points.

Table 1: Summary of normalization uncertainties

Source	Relative uncertainty (%)
Jet reconstruction and identification	1.8
Purity of Z+jet sample	1.6
Sum	2.4

Table 2: Summary of point-to-point uncertainties

Source	Relative uncertainty (%)
Track reconstruction efficiency	0.2 – 8.7
Particle Identification	0.8 – 15.0 ($\pi^{\pm}$), 0.1 – 34.6 ($K^{\pm}$), 0.5 – 52.5 ($p^{\pm}$)

Table 3: Summary of correlated uncertainties

Source	Relative uncertainty (%)
Jet energy scale	0.4 – 43.4
Jet energy resolution	3.8 – 48.3
Unfolding	1.4

Results of $f(z, j_{\mathrm{T}})$ at higher jet p_{T} intervals

The $f(z, j_{\mathrm{T}})$ measurements at higher jet p_{T} intervals comparing three different particle species are provided in Fig. 1 and Fig. 2. The trend of distributions for charged kaons and protons is similar to the one shown in charged pions.

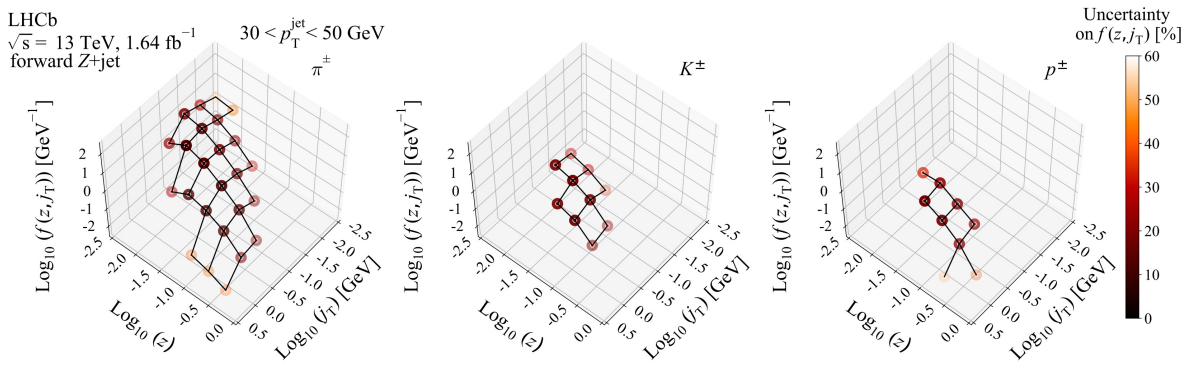

Figure 1: Joint distributions of the longitudinal momentum fraction z and the transverse momentum j_T of identified charged (left) pions, (middle) kaons and (right) protons in jets with $30 < p_T < 50$ GeV. Statistical (systematic) uncertainties are shown in bars (boxes).

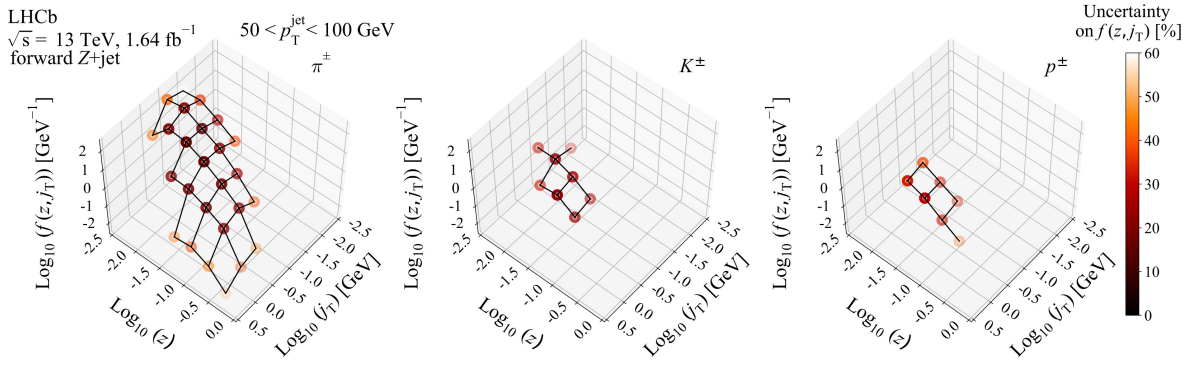

Figure 2: Joint distributions of the longitudinal momentum fraction z and the transverse momentum j_T of identified charged (left) pions, (middle) kaons and (right) protons in jets with $50 < p_T < 100$ GeV. Statistical (systematic) uncertainties are shown in bars (boxes).

Numerical Results

Numerical results are provided in Tables 4 – 15 for unidentified charged hadrons, charged pions, charged kaons, and charged protons. In addition to double differential jet fragmentation functions in z and j_T, single differential jet fragmentation functions $F(z)$ and $F(j_T)$ are shown separately in three jet p_T intervals as their uncertainties can be correlated between intervals.

Table 4: Summary of measured charged-hadron collinear jet fragmentation function $F(z)$ in three jet p_{T} intervals.

z	$F(z)$								
	$20 < p_{\mathrm{T}}^{\mathrm{jet}} < 30$ GeV			$30 < p_{\mathrm{T}}^{\mathrm{jet}} < 50$ GeV			$50 < p_{\mathrm{T}}^{\mathrm{jet}} < 100$ GeV		
$0.003 - 0.005$							26.5	$\pm$ 7.6	$\pm$ 15.8
$0.005 - 0.007$							81.0	$\pm$ 13.1	$\pm$ 21.1
$0.007 - 0.009$	5.68	$\pm$ 1.88	$\pm$ 2.13	37.7	$\pm$ 5.2	$\pm$ 9.0	153	$\pm$ 17	$\pm$ 27
$0.009 - 0.014$	21.3	$\pm$ 2.7	$\pm$ 3.4	79.2	$\pm$ 7.3	$\pm$ 10.4	182	$\pm$ 17	$\pm$ 25
$0.014 - 0.020$	45.1	$\pm$ 3.7	$\pm$ 4.8	110	$\pm$ 8	$\pm$ 13	159	$\pm$ 14	$\pm$ 22
$0.020 - 0.028$	67.7	$\pm$ 4.2	$\pm$ 7.5	106	$\pm$ 7	$\pm$ 9	124	$\pm$ 11	$\pm$ 17
$0.028 - 0.041$	63.5	$\pm$ 3.5	$\pm$ 7.3	82.4	$\pm$ 5.0	$\pm$ 8.8	88.9	$\pm$ 7.7	$\pm$ 12.3
$0.041 - 0.058$	47.5	$\pm$ 2.6	$\pm$ 4.4	55.1	$\pm$ 3.4	$\pm$ 6.7	58.3	$\pm$ 5.0	$\pm$ 7.8
$0.058 - 0.084$	31.2	$\pm$ 1.7	$\pm$ 2.4	33.6	$\pm$ 2.1	$\pm$ 3.6	32.7	$\pm$ 2.9	$\pm$ 4.1
$0.084 - 0.12$	19.1	$\pm$ 1.0	$\pm$ 1.4	20.8	$\pm$ 1.3	$\pm$ 1.7	18.7	$\pm$ 1.8	$\pm$ 2.5
$0.12 - 0.17$	10.5	$\pm$ 0.6	$\pm$ 1.0	11.4	$\pm$ 0.8	$\pm$ 1.0	10.4	$\pm$ 1.1	$\pm$ 1.6
$0.17 - 0.25$	5.49	$\pm$ 0.35	$\pm$ 0.78	6.06	$\pm$ 0.46	$\pm$ 0.58	5.13	$\pm$ 0.60	$\pm$ 0.79
$0.25 - 0.36$	2.42	$\pm$ 0.19	$\pm$ 0.29	2.55	$\pm$ 0.23	$\pm$ 0.24	2.20	$\pm$ 0.31	$\pm$ 0.35
$0.36 - 0.52$	0.776	$\pm$ 0.081	$\pm$ 0.101	0.947	$\pm$ 0.114	$\pm$ 0.101	0.705	$\pm$ 0.125	$\pm$ 0.124
$0.52 - 0.75$	0.225	$\pm$ 0.036	$\pm$ 0.039	0.260	$\pm$ 0.050	$\pm$ 0.032	0.141	$\pm$ 0.053	$\pm$ 0.029

Table 5: Summary of measured charged-hadron momentum transverse to the jet axis $F(j_{\mathrm{T}})$ in three jet p_{T} intervals.

j_{T}	$F(j_{\mathrm{T}})$								
	$20 < p_{\mathrm{T}}^{\mathrm{jet}} < 30$ GeV			$30 < p_{\mathrm{T}}^{\mathrm{jet}} < 50$ GeV			$50 < p_{\mathrm{T}}^{\mathrm{jet}} < 100$ GeV		
$0.010 - 0.016$				1.99	$\pm$ 0.75	$\pm$ 0.50			
$0.016 - 0.025$	1.95	$\pm$ 0.51	$\pm$ 0.53	2.70	$\pm$ 0.88	$\pm$ 0.60	4.38	$\pm$ 1.27	$\pm$ 0.90
$0.025 - 0.040$	3.41	$\pm$ 0.59	$\pm$ 0.86	4.23	$\pm$ 0.67	$\pm$ 0.59	4.84	$\pm$ 1.30	$\pm$ 0.79
$0.040 - 0.063$	5.14	$\pm$ 0.57	$\pm$ 1.01	7.30	$\pm$ 0.87	$\pm$ 0.57	6.92	$\pm$ 1.07	$\pm$ 0.95
$0.063 - 0.10$	7.70	$\pm$ 0.62	$\pm$ 1.07	9.84	$\pm$ 0.87	$\pm$ 0.85	10.0	$\pm$ 1.2	$\pm$ 0.9
$0.10 - 0.16$	10.5	$\pm$ 0.6	$\pm$ 0.8	13.4	$\pm$ 0.9	$\pm$ 1.6	13.1	$\pm$ 1.2	$\pm$ 1.0
$0.16 - 0.25$	12.0	$\pm$ 0.6	$\pm$ 0.9	14.7	$\pm$ 0.8	$\pm$ 1.4	15.2	$\pm$ 1.2	$\pm$ 1.5
$0.25 - 0.40$	9.35	$\pm$ 0.44	$\pm$ 0.81	11.5	$\pm$ 0.6	$\pm$ 0.9	13.2	$\pm$ 1.0	$\pm$ 1.6
$0.40 - 0.63$	5.06	$\pm$ 0.25	$\pm$ 0.46	6.36	$\pm$ 0.35	$\pm$ 0.55	7.44	$\pm$ 0.57	$\pm$ 0.98
$0.63 - 1.0$	1.64	$\pm$ 0.10	$\pm$ 0.23	2.40	$\pm$ 0.15	$\pm$ 0.16	3.06	$\pm$ 0.26	$\pm$ 0.40
$1.0 - 1.6$	0.250	$\pm$ 0.024	$\pm$ 0.071	0.510	$\pm$ 0.046	$\pm$ 0.077	0.759	$\pm$ 0.082	$\pm$ 0.108
$1.6 - 2.5$	0.018	$\pm$ 0.005	$\pm$ 0.011	0.056	$\pm$ 0.008	$\pm$ 0.022	0.126	$\pm$ 0.021	$\pm$ 0.041

Table 6: Summary of measured charged-hadron transverse momentum dependent jet fragmentation function $f(z, j_T)$ in three jet p_T intervals.

j_T / z	$f(z, j_T)$		
	$20 < p_T^{jet} < 30$ GeV	$30 < p_T^{jet} < 50$ GeV	$50 < p_T^{jet} < 100$ GeV
0.01 – 0.03		93.3 ± 33.3 ± 38.9	
0.007 – 0.015			
0.01 – 0.03	41.7 ± 13.3 ± 17.6	65.1 ± 21.6 ± 17.4	
0.015 – 0.033			
0.01 – 0.03	11.4 ± 4.0 ± 3.8		
0.033 – 0.072			
0.03 – 0.07			208 ± 55 ± 121
0.003 – 0.007			
0.03 – 0.07	82.9 ± 16.8 ± 19.8	198 ± 33 ± 41	305 ± 66 ± 89
0.007 – 0.015			
0.03 – 0.07	104 ± 13 ± 27	128 ± 18 ± 17	110 ± 23 ± 16
0.015 – 0.033			
0.03 – 0.07	36.1 ± 5.5 ± 10.5	39.5 ± 6.9 ± 4.2	27.9 ± 8.5 ± 5.3
0.033 – 0.072			
0.03 – 0.07	7.57 ± 2.00 ± 1.36	7.37 ± 1.90 ± 1.12	
0.072 – 0.16			
0.03 – 0.07	1.46 ± 0.48 ± 0.29		
0.16 – 0.34			
0.07 – 0.19			361 ± 62 ± 136
0.003 – 0.007			
0.07 – 0.19	110 ± 13 ± 19	340 ± 30 ± 52	519 ± 55 ± 93
0.007 – 0.015			
0.07 – 0.19	225 ± 15 ± 19	255 ± 19 ± 29	195 ± 21 ± 21
0.015 – 0.033			
0.07 – 0.19	80.6 ± 5.8 ± 7.5	83.0 ± 6.8 ± 12.6	66.3 ± 8.9 ± 10.1
0.033 – 0.072			
0.07 – 0.19	18.2 ± 1.6 ± 2.1	18.5 ± 2.0 ± 2.1	12.1 ± 2.1 ± 1.8
0.072 – 0.16			
0.07 – 0.19	3.03 ± 0.38 ± 0.48	3.02 ± 0.49 ± 0.42	1.53 ± 0.46 ± 0.26
0.16 – 0.34			
0.07 – 0.19	0.270 ± 0.086 ± 0.067		
0.34 – 0.75			

Continued on next page

j_T / z	$f(z, j_T)$		
	$20 < p_T^{jet} < 30$ GeV	$30 < p_T^{jet} < 50$ GeV	$50 < p_T^{jet} < 100$ GeV
0.19 − 0.52			32.3 ± 9.8 ± 9.4
0.003 − 0.007			
0.19 − 0.52		59.9 ± 8.5 ± 10.2	278 ± 26 ± 49
0.007 − 0.015			
0.19 − 0.52	91.9 ± 5.8 ± 10.9	185 ± 11 ± 20	218 ± 18 ± 31
0.015 − 0.033			
0.19 − 0.52	87.8 ± 4.4 ± 9.1	87.5 ± 5.1 ± 11.3	76.4 ± 6.7 ± 10.0
0.033 − 0.072			
0.19 − 0.52	26.0 ± 1.4 ± 1.8	25.6 ± 1.7 ± 2.4	21.5 ± 2.2 ± 3.1
0.072 − 0.16			
0.19 − 0.52	5.88 ± 0.40 ± 0.66	5.73 ± 0.49 ± 0.56	4.19 ± 0.56 ± 0.67
0.16 − 0.34			
0.19 − 0.52	0.576 ± 0.079 ± 0.094	0.445 ± 0.077 ± 0.047	0.080 ± 0.032 ± 0.012
0.34 − 0.75			
0.52 − 1.4			3.33 ± 1.17 ± 0.67
0.007 − 0.015			
0.52 − 1.4		5.63 ± 1.19 ± 0.49	27.7 ± 3.3 ± 4.5
0.015 − 0.033			
0.52 − 1.4	6.68 ± 0.62 ± 1.44	15.2 ± 1.2 ± 1.5	23.3 ± 2.2 ± 3.7
0.033 − 0.072			
0.52 − 1.4	6.84 ± 0.42 ± 0.80	8.06 ± 0.56 ± 0.68	8.25 ± 0.85 ± 1.14
0.072 − 0.16			
0.52 − 1.4	2.16 ± 0.15 ± 0.29	2.47 ± 0.20 ± 0.22	2.00 ± 0.25 ± 0.33
0.16 − 0.34			
0.52 − 1.4	0.287 ± 0.032 ± 0.036	0.291 ± 0.037 ± 0.028	0.049 ± 0.014 ± 0.009
0.34 − 0.75			
1.4 − 3.7			0.481 ± 0.137 ± 0.121
0.033 − 0.072			
1.4 − 3.7		0.191 ± 0.040 ± 0.061	0.497 ± 0.103 ± 0.145
0.072 − 0.16			
1.4 − 3.7	0.040 ± 0.011 ± 0.024	0.092 ± 0.015 ± 0.036	0.131 ± 0.032 ± 0.044
0.16 − 0.34			
1.4 − 3.7	0.014 ± 0.005 ± 0.006	0.021 ± 0.006 ± 0.006	0.011 ± 0.004 ± 0.004
0.34 − 0.75			

Table 7: Summary of measured charged-pion collinear jet fragmentation function $F(z)$ in three jet p_{T} intervals.

z	$F(z)$		
	$20 < p_{\mathrm{T}}^{\mathrm{jet}} < 30$ GeV	$30 < p_{\mathrm{T}}^{\mathrm{jet}} < 50$ GeV	$50 < p_{\mathrm{T}}^{\mathrm{jet}} < 100$ GeV
$0.003 - 0.005$			$22.9 \pm 6.5 \pm 13.7$
$0.005 - 0.007$			$66.0 \pm 10.7 \pm 17.6$
$0.007 - 0.009$	$6.11 \pm 2.02 \pm 2.30$	$35.3 \pm 4.9 \pm 8.8$	$119 \pm 13 \pm 22$
$0.009 - 0.014$	$22.7 \pm 2.9 \pm 3.9$	$69.7 \pm 6.5 \pm 10.5$	$132 \pm 13 \pm 19$
$0.014 - 0.020$	$49.2 \pm 4.1 \pm 6.5$	$90.1 \pm 6.3 \pm 11.9$	$111 \pm 10 \pm 16$
$0.020 - 0.028$	$72.9 \pm 4.7 \pm 10.4$	$85.9 \pm 5.7 \pm 8.3$	$85.2 \pm 7.7 \pm 11.7$
$0.028 - 0.041$	$63.5 \pm 3.6 \pm 8.8$	$64.9 \pm 4.1 \pm 7.2$	$62.6 \pm 5.8 \pm 8.7$
$0.041 - 0.058$	$44.2 \pm 2.5 \pm 4.8$	$42.4 \pm 2.7 \pm 5.2$	$39.8 \pm 3.6 \pm 5.3$
$0.058 - 0.084$	$26.9 \pm 1.5 \pm 2.3$	$25.0 \pm 1.6 \pm 2.7$	$23.3 \pm 2.3 \pm 2.9$
$0.084 - 0.12$	$15.6 \pm 0.9 \pm 1.2$	$14.9 \pm 1.0 \pm 1.2$	$12.5 \pm 1.4 \pm 1.7$
$0.12 - 0.17$	$8.58 \pm 0.56 \pm 0.81$	$7.70 \pm 0.58 \pm 0.72$	$7.42 \pm 0.83 \pm 1.23$
$0.17 - 0.25$	$4.34 \pm 0.30 \pm 0.62$	$4.19 \pm 0.37 \pm 0.44$	$4.08 \pm 0.51 \pm 0.73$
$0.25 - 0.36$	$2.00 \pm 0.18 \pm 0.26$	$2.00 \pm 0.20 \pm 0.23$	$1.92 \pm 0.29 \pm 0.39$
$0.36 - 0.52$	$0.723 \pm 0.087 \pm 0.115$	$0.827 \pm 0.106 \pm 0.119$	$0.690 \pm 0.127 \pm 0.160$
$0.52 - 0.75$	$0.241 \pm 0.045 \pm 0.052$	$0.256 \pm 0.050 \pm 0.045$	$0.149 \pm 0.056 \pm 0.039$

Table 8: Summary of measured charged-pion momentum transverse to the jet axis $F(j_{\mathrm{T}})$ in three jet p_{T} intervals.

j_{T}	$F(j_{\mathrm{T}})$		
	$20 < p_{\mathrm{T}}^{\mathrm{jet}} < 30$ GeV	$30 < p_{\mathrm{T}}^{\mathrm{jet}} < 50$ GeV	$50 < p_{\mathrm{T}}^{\mathrm{jet}} < 100$ GeV
$0.010 - 0.016$		$2.02 \pm 0.77 \pm 0.51$	
$0.016 - 0.025$	$2.24 \pm 0.64 \pm 0.64$	$2.60 \pm 0.88 \pm 0.58$	$3.08 \pm 0.90 \pm 0.70$
$0.025 - 0.040$	$3.87 \pm 0.68 \pm 1.00$	$3.87 \pm 0.64 \pm 0.55$	$3.46 \pm 1.01 \pm 0.61$
$0.040 - 0.063$	$5.27 \pm 0.61 \pm 1.06$	$6.12 \pm 0.74 \pm 0.50$	$4.98 \pm 0.80 \pm 0.71$
$0.063 - 0.10$	$7.64 \pm 0.65 \pm 1.12$	$8.20 \pm 0.75 \pm 0.77$	$7.85 \pm 0.98 \pm 0.69$
$0.10 - 0.16$	$10.4 \pm 0.6 \pm 1.0$	$10.8 \pm 0.7 \pm 1.3$	$10.5 \pm 1.0 \pm 0.8$
$0.16 - 0.25$	$11.9 \pm 0.6 \pm 1.3$	$12.0 \pm 0.7 \pm 1.3$	$12.1 \pm 1.0 \pm 1.2$
$0.25 - 0.40$	$8.69 \pm 0.43 \pm 0.87$	$9.27 \pm 0.51 \pm 0.80$	$9.97 \pm 0.77 \pm 1.26$
$0.40 - 0.63$	$4.15 \pm 0.22 \pm 0.40$	$4.64 \pm 0.27 \pm 0.41$	$5.17 \pm 0.42 \pm 0.71$
$0.63 - 1.0$	$1.27 \pm 0.08 \pm 0.19$	$1.58 \pm 0.11 \pm 0.12$	$1.85 \pm 0.17 \pm 0.25$
$1.0 - 1.6$	$0.211 \pm 0.024 \pm 0.061$	$0.320 \pm 0.034 \pm 0.051$	$0.400 \pm 0.050 \pm 0.059$
$1.6 - 2.5$	$0.019 \pm 0.007 \pm 0.012$	$0.038 \pm 0.007 \pm 0.016$	$0.061 \pm 0.012 \pm 0.020$

Table 9: Summary of measured charged-pion transverse momentum dependent jet fragmentation function $f(z, j_{\mathrm{T}})$ in three jet p_{T} intervals.

j_{T} / z	$f(z, j_{\mathrm{T}})$		
	$20 < p_{\mathrm{T}}^{\mathrm{jet}} < 30$ GeV	$30 < p_{\mathrm{T}}^{\mathrm{jet}} < 50$ GeV	$50 < p_{\mathrm{T}}^{\mathrm{jet}} < 100$ GeV
0.01 − 0.03		85.3 ± 30.6 ± 35.7	
0.007 − 0.015			
0.01 − 0.03	52.1 ± 17.3 ± 22.6	65.6 ± 22.7 ± 17.7	
0.015 − 0.033			
0.01 − 0.03	13.7 ± 5.0 ± 4.8		
0.033 − 0.072			
0.03 − 0.07			170 ± 45 ± 99
0.003 − 0.007			
0.03 − 0.07	84.1 ± 17.0 ± 20.4	167 ± 28 ± 36	211 ± 47 ± 61
0.007 − 0.015			
0.03 − 0.07	109 ± 14 ± 29	109 ± 15 ± 15	75.1 ± 18.3 ± 12.6
0.015 − 0.033			
0.03 − 0.07	39.5 ± 6.3 ± 11.8	34.2 ± 6.6 ± 3.7	22.6 ± 7.2 ± 4.9
0.033 − 0.072			
0.03 − 0.07	7.63 ± 2.16 ± 1.38	6.16 ± 1.66 ± 0.96	
0.072 − 0.16			
0.03 − 0.07	1.28 ± 0.47 ± 0.26		
0.16 − 0.34			
0.07 − 0.19			307 ± 53 ± 118
0.003 − 0.007			
0.07 − 0.19	118 ± 14 ± 21	307 ± 27 ± 52	424 ± 46 ± 78
0.007 − 0.015			
0.07 − 0.19	239 ± 16 ± 27	207 ± 16 ± 26	144 ± 16 ± 16
0.015 − 0.033			
0.07 − 0.19	79.0 ± 6.0 ± 8.7	65.1 ± 5.6 ± 10.0	53.2 ± 7.6 ± 8.7
0.033 − 0.072			
0.07 − 0.19	15.8 ± 1.5 ± 1.9	14.2 ± 1.7 ± 1.6	9.80 ± 1.94 ± 1.53
0.072 − 0.16			
0.07 − 0.19	2.50 ± 0.36 ± 0.41	1.96 ± 0.36 ± 0.29	1.19 ± 0.41 ± 0.22
0.16 − 0.34			

Continued on next page

j_T / z	$f(z, j_T)$		
	$20 < p_T^{jet} < 30$ GeV	$30 < p_T^{jet} < 50$ GeV	$50 < p_T^{jet} < 100$ GeV
0.19 − 0.52			23.9 ± 7.3 ± 7.1
0.003 − 0.007			
0.19 − 0.52		50.3 ± 7.2 ± 9.4	194 ± 19 ± 35
0.007 − 0.015			
0.19 − 0.52	98.1 ± 6.4 ± 15.5	152 ± 9 ± 18	159 ± 14 ± 23
0.015 − 0.033			
0.19 − 0.52	82.5 ± 4.3 ± 10.0	72.5 ± 4.4 ± 9.5	60.1 ± 5.5 ± 7.9
0.033 − 0.072			
0.19 − 0.52	21.4 ± 1.2 ± 1.5	19.3 ± 1.3 ± 1.8	16.4 ± 1.8 ± 2.3
0.072 − 0.16			
0.19 − 0.52	4.65 ± 0.35 ± 0.53	4.07 ± 0.40 ± 0.43	3.43 ± 0.49 ± 0.61
0.16 − 0.34			
0.19 − 0.52	0.532 ± 0.089 ± 0.097	0.346 ± 0.064 ± 0.047	0.081 ± 0.034 ± 0.015
0.34 − 0.75			
0.52 − 1.4		3.06 ± 0.82 ± 0.27	14.5 ± 2.0 ± 2.4
0.015 − 0.033			
0.52 − 1.4	4.94 ± 0.53 ± 1.10	9.28 ± 0.83 ± 0.91	12.8 ± 1.3 ± 2.1
0.033 − 0.072			
0.52 − 1.4	5.36 ± 0.38 ± 0.64	5.29 ± 0.41 ± 0.45	5.36 ± 0.63 ± 0.75
0.072 − 0.16			
0.52 − 1.4	1.74 ± 0.13 ± 0.24	1.77 ± 0.16 ± 0.18	1.65 ± 0.22 ± 0.32
0.16 − 0.34			
0.52 − 1.4	0.277 ± 0.034 ± 0.045	0.256 ± 0.035 ± 0.033	0.047 ± 0.014 ± 0.011
0.34 − 0.75			
1.4 − 3.7			0.174 ± 0.060 ± 0.044
0.033 − 0.072			
1.4 − 3.7		0.109 ± 0.027 ± 0.035	0.216 ± 0.053 ± 0.063
0.072 − 0.16			
1.4 − 3.7		0.059 ± 0.012 ± 0.023	0.079 ± 0.021 ± 0.027
0.16 − 0.34			
1.4 − 3.7	0.018 ± 0.006 ± 0.007	0.022 ± 0.007 ± 0.006	0.009 ± 0.003 ± 0.003
0.34 − 0.75			

Table 10: Summary of measured charged-kaon collinear jet fragmentation function $F(z)$ in three jet p_{T} intervals.

z	$F(z)$		
	$20 < p_{\mathrm{T}}^{\mathrm{jet}} < 30$ GeV	$30 < p_{\mathrm{T}}^{\mathrm{jet}} < 50$ GeV	$50 < p_{\mathrm{T}}^{\mathrm{jet}} < 100$ GeV
$0.009 - 0.014$			$11.8 \pm 3.2 \pm 3.4$
$0.014 - 0.020$		$5.53 \pm 1.39 \pm 1.93$	$12.2 \pm 2.6 \pm 2.8$
$0.020 - 0.028$	$2.89 \pm 0.52 \pm 1.05$	$7.12 \pm 1.14 \pm 1.66$	$13.5 \pm 2.5 \pm 2.6$
$0.028 - 0.041$	$4.66 \pm 0.67 \pm 1.13$	$7.31 \pm 1.18 \pm 1.13$	$11.8 \pm 2.2 \pm 2.1$
$0.041 - 0.058$	$4.71 \pm 0.61 \pm 0.60$	$6.52 \pm 1.01 \pm 0.84$	$10.9 \pm 2.2 \pm 1.9$
$0.058 - 0.084$	$3.92 \pm 0.44 \pm 0.31$	$4.76 \pm 0.66 \pm 0.54$	$5.15 \pm 0.99 \pm 0.92$
$0.084 - 0.12$	$2.76 \pm 0.33 \pm 0.21$	$3.22 \pm 0.45 \pm 0.34$	$3.30 \pm 0.66 \pm 0.77$
$0.12 - 0.17$	$1.52 \pm 0.19 \pm 0.18$	$1.72 \pm 0.25 \pm 0.27$	$1.28 \pm 0.31 \pm 0.39$
$0.17 - 0.25$	$0.678 \pm 0.092 \pm 0.125$	$0.622 \pm 0.099 \pm 0.122$	
$0.25 - 0.36$	$0.247 \pm 0.047 \pm 0.049$	$0.174 \pm 0.047 \pm 0.041$	
$0.36 - 0.52$	$0.044 \pm 0.012 \pm 0.009$		

Table 11: Summary of measured charged-kaon momentum transverse to the jet axis $F(j_{\mathrm{T}})$ in three jet p_{T} intervals.

j_{T}	$F(j_{\mathrm{T}})$		
	$20 < p_{\mathrm{T}}^{\mathrm{jet}} < 30$ GeV	$30 < p_{\mathrm{T}}^{\mathrm{jet}} < 50$ GeV	$50 < p_{\mathrm{T}}^{\mathrm{jet}} < 100$ GeV
$0.063 - 0.10$	$0.409 \pm 0.108 \pm 0.073$	$0.365 \pm 0.126 \pm 0.046$	
$0.10 - 0.16$	$0.596 \pm 0.104 \pm 0.081$	$0.713 \pm 0.144 \pm 0.117$	
$0.16 - 0.25$	$0.793 \pm 0.095 \pm 0.106$	$0.891 \pm 0.134 \pm 0.135$	$1.02 \pm 0.19 \pm 0.20$
$0.25 - 0.40$	$0.884 \pm 0.089 \pm 0.113$	$1.09 \pm 0.13 \pm 0.15$	$1.23 \pm 0.20 \pm 0.24$
$0.40 - 0.63$	$0.693 \pm 0.062 \pm 0.081$	$0.863 \pm 0.090 \pm 0.113$	$1.04 \pm 0.15 \pm 0.20$
$0.63 - 1.0$	$0.238 \pm 0.028 \pm 0.042$	$0.380 \pm 0.050 \pm 0.054$	$0.621 \pm 0.103 \pm 0.133$
$1.0 - 1.6$	$0.040 \pm 0.009 \pm 0.013$	$0.087 \pm 0.018 \pm 0.020$	$0.161 \pm 0.036 \pm 0.043$
$1.6 - 2.5$		$0.008 \pm 0.003 \pm 0.003$	

Table 12: Summary of measured charged-kaon transverse momentum dependent jet fragmentation function $f(z, j_{\mathrm{T}})$ in three jet p_{T} intervals.

j_{T} / z	$f(z, j_{\mathrm{T}})$		
	$20 < p_{\mathrm{T}}^{\mathrm{jet}} < 30$ GeV	$30 < p_{\mathrm{T}}^{\mathrm{jet}} < 50$ GeV	$50 < p_{\mathrm{T}}^{\mathrm{jet}} < 100$ GeV
0.07 − 0.19	6.88 ± 1.63 ± 2.37	10.2 ± 2.8 ± 2.9	13.7 ± 4.2 ± 2.4
0.015 − 0.033			
0.07 − 0.19	5.42 ± 1.07 ± 0.71	5.65 ± 1.37 ± 0.86	
0.033 − 0.072			
0.07 − 0.19	1.81 ± 0.37 ± 0.21	1.80 ± 0.58 ± 0.21	
0.072 − 0.16			
0.19 − 0.52			20.5 ± 5.3 ± 6.3
0.007 − 0.015			
0.19 − 0.52	5.27 ± 0.97 ± 1.85	14.5 ± 2.1 ± 3.9	20.8 ± 3.8 ± 4.3
0.015 − 0.033			
0.19 − 0.52	8.54 ± 0.94 ± 1.36	8.69 ± 1.35 ± 1.24	9.53 ± 2.05 ± 1.63
0.033 − 0.072			
0.19 − 0.52	3.45 ± 0.42 ± 0.24	3.28 ± 0.49 ± 0.32	2.53 ± 0.58 ± 0.51
0.072 − 0.16			
0.19 − 0.52	0.673 ± 0.106 ± 0.089	0.512 ± 0.107 ± 0.074	
0.16 − 0.34			
0.19 − 0.52	0.039 ± 0.014 ± 0.008		
0.34 − 0.75			
0.52 − 1.4			4.76 ± 1.39 ± 1.01
0.015 − 0.033			
0.52 − 1.4	1.06 ± 0.21 ± 0.24	2.91 ± 0.49 ± 0.35	6.03 ± 1.12 ± 1.22
0.033 − 0.072			
0.52 − 1.4	1.20 ± 0.15 ± 0.15	1.53 ± 0.22 ± 0.21	1.57 ± 0.31 ± 0.40
0.072 − 0.16			
0.52 − 1.4	0.250 ± 0.038 ± 0.052	0.266 ± 0.049 ± 0.060	
0.16 − 0.34			
0.52 − 1.4	0.012 ± 0.004 ± 0.003		
0.34 − 0.75			

Table 13: Summary of measured charged-proton collinear jet fragmentation function $F(z)$ in three jet p_{T} intervals.

z	$F(z)$		
	$20 < p_{\mathrm{T}}^{\mathrm{jet}} < 30$ GeV	$30 < p_{\mathrm{T}}^{\mathrm{jet}} < 50$ GeV	$50 < p_{\mathrm{T}}^{\mathrm{jet}} < 100$ GeV
$0.014 - 0.020$			$10.2 \pm 3.8 \pm 1.4$
$0.020 - 0.028$			$13.0 \pm 4.4 \pm 1.8$
$0.028 - 0.041$	$2.31 \pm 0.84 \pm 0.27$	$6.77 \pm 1.32 \pm 1.07$	$9.60 \pm 2.27 \pm 1.32$
$0.041 - 0.058$	$2.84 \pm 0.72 \pm 0.31$	$6.21 \pm 1.01 \pm 0.93$	$6.02 \pm 1.82 \pm 0.84$
$0.058 - 0.084$	$3.34 \pm 0.48 \pm 0.33$	$4.32 \pm 0.66 \pm 0.57$	$3.43 \pm 0.78 \pm 0.52$
$0.084 - 0.12$	$2.00 \pm 0.28 \pm 0.21$	$2.59 \pm 0.45 \pm 0.36$	$2.55 \pm 0.62 \pm 0.61$
$0.12 - 0.17$	$1.10 \pm 0.17 \pm 0.11$	$1.58 \pm 0.27 \pm 0.29$	$1.54 \pm 0.48 \pm 0.54$
$0.17 - 0.25$	$0.658 \pm 0.117 \pm 0.107$	$0.857 \pm 0.146 \pm 0.221$	$0.854 \pm 0.284 \pm 0.409$
$0.25 - 0.36$	$0.238 \pm 0.043 \pm 0.040$	$0.237 \pm 0.058 \pm 0.091$	$0.307 \pm 0.103 \pm 0.168$
$0.36 - 0.52$	$0.068 \pm 0.019 \pm 0.013$		

Table 14: Summary of measured charged-proton momentum transverse to the jet axis $F(j_{\mathrm{T}})$ in three jet p_{T} intervals.

j_{T}	$F(j_{\mathrm{T}})$		
	$20 < p_{\mathrm{T}}^{\mathrm{jet}} < 30$ GeV	$30 < p_{\mathrm{T}}^{\mathrm{jet}} < 50$ GeV	$50 < p_{\mathrm{T}}^{\mathrm{jet}} < 100$ GeV
$0.10 - 0.16$	$0.217 \pm 0.070 \pm 0.022$	$0.305 \pm 0.109 \pm 0.038$	$0.298 \pm 0.115 \pm 0.043$
$0.16 - 0.25$	$0.457 \pm 0.093 \pm 0.038$	$0.460 \pm 0.091 \pm 0.057$	$0.499 \pm 0.169 \pm 0.071$
$0.25 - 0.40$	$0.611 \pm 0.089 \pm 0.053$	$0.624 \pm 0.101 \pm 0.085$	$0.768 \pm 0.187 \pm 0.110$
$0.40 - 0.63$	$0.429 \pm 0.057 \pm 0.058$	$0.740 \pm 0.098 \pm 0.143$	$0.836 \pm 0.154 \pm 0.114$
$0.63 - 1.0$	$0.290 \pm 0.036 \pm 0.058$	$0.481 \pm 0.060 \pm 0.081$	$0.610 \pm 0.123 \pm 0.106$
$1.0 - 1.6$	$0.052 \pm 0.011 \pm 0.017$	$0.143 \pm 0.029 \pm 0.033$	$0.178 \pm 0.048 \pm 0.052$
$1.6 - 2.5$			$0.043 \pm 0.015 \pm 0.023$

Table 15: Summary of measured charged-proton transverse momentum dependent jet fragmentation function $f(z, j_{\mathrm{T}})$ in three jet p_{T} intervals.

j_{T} / z	$f(z, j_{\mathrm{T}})$		
	$20 < p_{\mathrm{T}}^{\mathrm{jet}} < 30$ GeV	$30 < p_{\mathrm{T}}^{\mathrm{jet}} < 50$ GeV	$50 < p_{\mathrm{T}}^{\mathrm{jet}} < 100$ GeV
0.07 − 0.19	$0.879 \pm 0.308 \pm 0.139$		
0.072 − 0.16			
0.07 − 0.19	$0.181 \pm 0.064 \pm 0.029$		
0.16 − 0.34			
0.19 − 0.52		$5.53 \pm 1.74 \pm 0.89$	$13.3 \pm 4.7 \pm 1.9$
0.015 − 0.033			
0.19 − 0.52	$5.51 \pm 1.08 \pm 0.58$	$6.40 \pm 1.25 \pm 1.00$	$4.88 \pm 1.50 \pm 0.65$
0.033 − 0.072			
0.19 − 0.52	$1.89 \pm 0.30 \pm 0.13$	$1.95 \pm 0.35 \pm 0.22$	$1.89 \pm 0.56 \pm 0.33$
0.072 − 0.16			
0.19 − 0.52	$0.600 \pm 0.116 \pm 0.070$	$0.641 \pm 0.139 \pm 0.158$	
0.16 − 0.34			
0.19 − 0.52	$0.050 \pm 0.016 \pm 0.010$		
0.34 − 0.75			
0.52 − 1.4			$8.33 \pm 2.42 \pm 1.41$
0.015 − 0.033			
0.52 − 1.4	$1.09 \pm 0.31 \pm 0.28$	$4.12 \pm 0.65 \pm 0.64$	$4.05 \pm 0.99 \pm 0.67$
0.033 − 0.072			
0.52 − 1.4	$1.22 \pm 0.16 \pm 0.20$	$1.52 \pm 0.25 \pm 0.26$	$1.08 \pm 0.32 \pm 0.26$
0.072 − 0.16			
0.52 − 1.4	$0.280 \pm 0.049 \pm 0.053$	$0.328 \pm 0.062 \pm 0.101$	$0.317 \pm 0.115 \pm 0.155$
0.16 − 0.34			
0.52 − 1.4	$0.021 \pm 0.007 \pm 0.005$	$0.024 \pm 0.009 \pm 0.013$	
0.34 − 0.75			
1.4 − 3.7		$0.028 \pm 0.010 \pm 0.011$	
0.16 − 0.34			